

Figure S1

Figure S1, related to STAR Methods, Experimental Model and Subject Details. PILO-SE mice exhibit hippocampal neurodegeneration with relative survival of the CA2 subfield and dentate gyrus. (A, B) Representative sections from PILO-SE mice used for *in vivo* chemogenetic experiments, stained with Cresyl Violet. The extent of neuronal depletion varies across the hippocampal subfields and is most severe in distal CA3 (adjacent to CA2) and the mid-to-distal CA1 (towards the subiculum). **(C)** A representative section from the cohort of mice used for *ex vivo* hippocampal slice recordings, stained for the Nissl substance. Severe neuronal depletion is visible in distal CA3 and the middle of CA1. Scale bars for all images are 200 μm .

Supplemental Table 1. CA2 pyramidal cell intrinsic physiological properties

Parameter	Control	PILO-SE
Resting membrane potential (mV)	-69.34 ± 0.4136	-69.16 ± 0.3439
Input resistance (mOhm)	50.38 ± 1.203	57.05 ± 1.458 (***P = 0.0009)
Membrane time constant (ms)	15.02 ± 0.3872	14.52 ± 0.3043
Membrane capacitance (pF)	300 ± 6.047	263.4 ± 6.884 (***P = 0.0005)
Hyperpolarization-activated voltage sag ratio	0.144 ± 0.0037	0.1711 ± 0.0052 (****P < 0.0001)
Action potential amplitude (mV)	92.21 ± 0.8607	91.62 ± 0.8611
Action potential half-width (ms)	0.9652 ± 0.01633	0.9838 ± 0.01396
Action potential maximum rate of rise (V.s)	398.3 ± 8.132	401 ± 7.553
Action potential maximum rate of descent (V.s)	-89.17 ± 1.703	-85.43 ± 1.450
Action potential afterhyperpolarization (mV)	-7.577 ± 0.1761	-8.652 ± 0.1829 (****P < 0.0001)
Action potential voltage threshold (mV)	-41.78 ± 0.5022	-42.01 ± 0.4717
Rheobase current (pA)	608.3 ± 13.34	558.0 ± 11.50 (**P = 0.0072)
Maximum current-evoked firing rate (Hz)	17.16 ± 0.6439	22.34 ± 0.4868 (****P < 0.0001)
Slow ramping depolarization, from initial V _m of -56 mV (mV)	3.605 ± 0.217	4.521 ± 0.189 (*P = 0.0174)

Supplemental Table 1, related to Figure 1. A summary of the intrinsic electrophysiological properties of CA2 PCs. Comparisons between CA2 PCs in hippocampal slices from control and PILO-SE mice revealed significant differences in several parameters. The membrane capacitance and rheobase current were decreased in cells from PILO-SE mice, whereas the input resistance, maximum firing rate, hyperpolarization-activated voltage sag ratio, action potential afterhyperpolarization, and slow ramping depolarization were all increased in CA2 PCs from PILO-SE mice relative to controls.

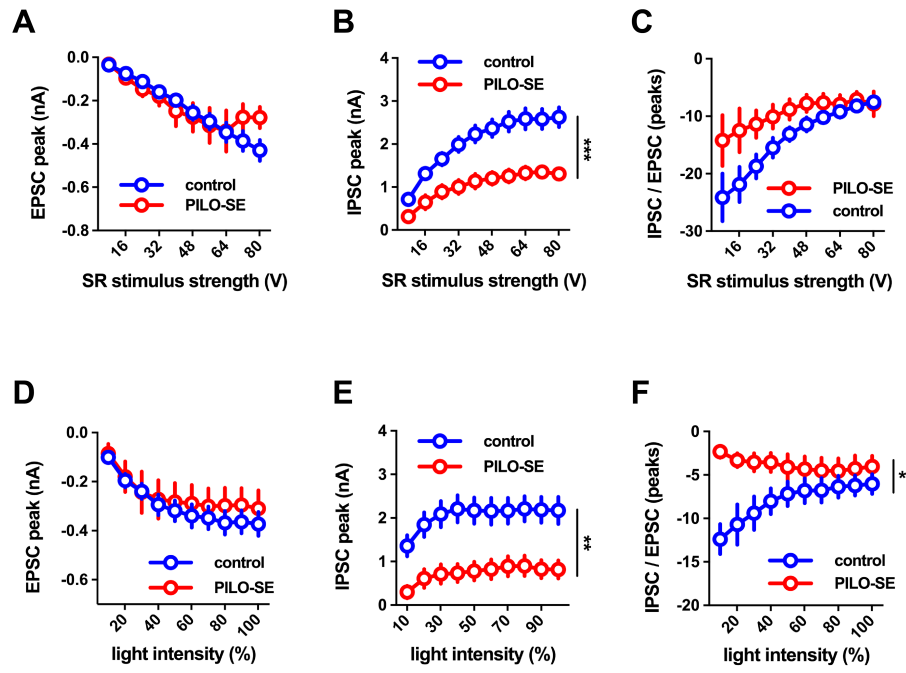


Figure S2

Figure S2, related to Figure 2 and Figure 3. The peak amplitude of inhibitory postsynaptic currents evoked in CA2 PCs by stimulation of CA2 and CA3 axons was reduced in slices from PILO-SE mice, whereas excitatory postsynaptic currents were unaltered. (A) Input-output curve of SR stimulus strength and the EPSC peak amplitude. **(B)** Input-output curve of SR stimulus strength and the IPSC peak amplitude. SR-evoked IPSC amplitude is reduced in CA2 PCs from PILO-SE mice. **(C)** Input-output curve of SR stimulus strength and the ratio of IPSC and EPSC peak amplitudes. **(D)** Input-output curve of photostimulation strength and the EPSC peak amplitude in intermediate CA2 PCs from Amigo2-Cre mice expressing ChR2-eYFP in dorsal CA2 PCs. **(E)** Input-output curve of photostimulation strength and the IPSC peak amplitude. Light-evoked IPSC amplitude is reduced in CA2 PCs from PILO-SE mice. **(F)** Input-output curve of photostimulation strength and the ratio of IPSC and EPSC peak amplitudes. The IPSC/EPSC peak ratio is reduced in CA2 PCs from PILO-SE mice (mixed-effects model; $*P = 0.0427$; $n = 14$ cells from 8 control mice, 9 cells from 4 PILO-SE mice).

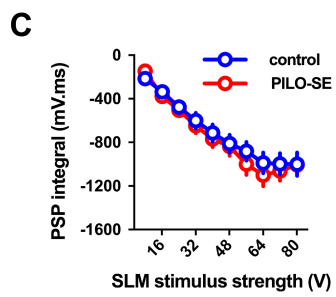
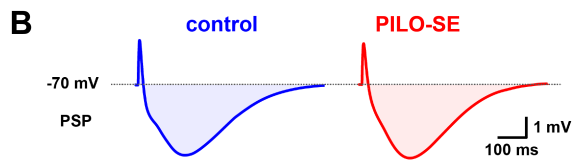
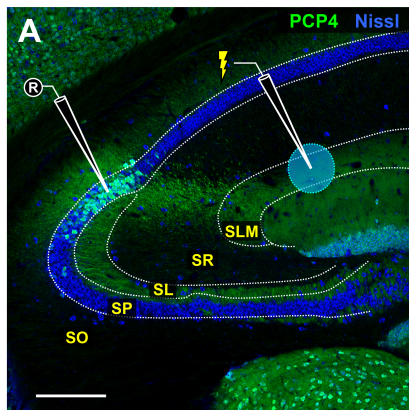


Figure S3

Figure S3, related to Figure 2. Inhibition in CA2 PCs elicited by activation of the EC LII inputs was not significantly altered in PILO-SE mice. (A) Representative hippocampal section stained for Nissl (blue) and PCP4 (green) to illustrate the configuration used to measure synaptic input to CA2 PCs from the EC LII projections in the SLM. Scale bar is 250 μm . **(B)** Representative averaged PSPs evoked by electrical stimulation in the SLM recorded in CA2 PCs from control (left, blue) and PILO-SE (right, red) mice. **(C)** The integral of the SLM-evoked PSP was not significantly different between the control and PILO-SE groups (mixed-effects model with Holm-Sidak's test; $P = 0.7934$; $n = 34$ cells from 21 control mice, 31 cells from 16 PILO-SE mice).

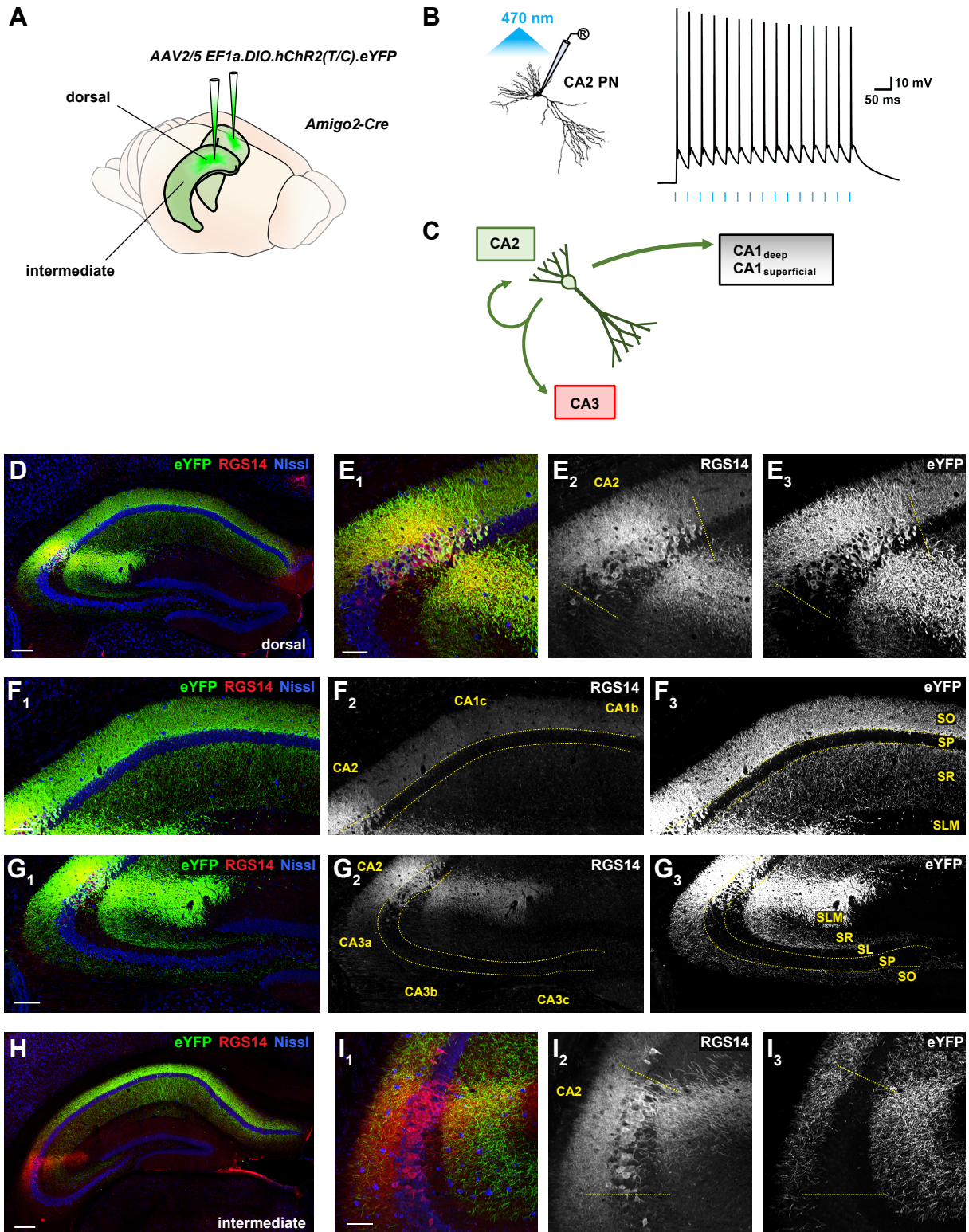
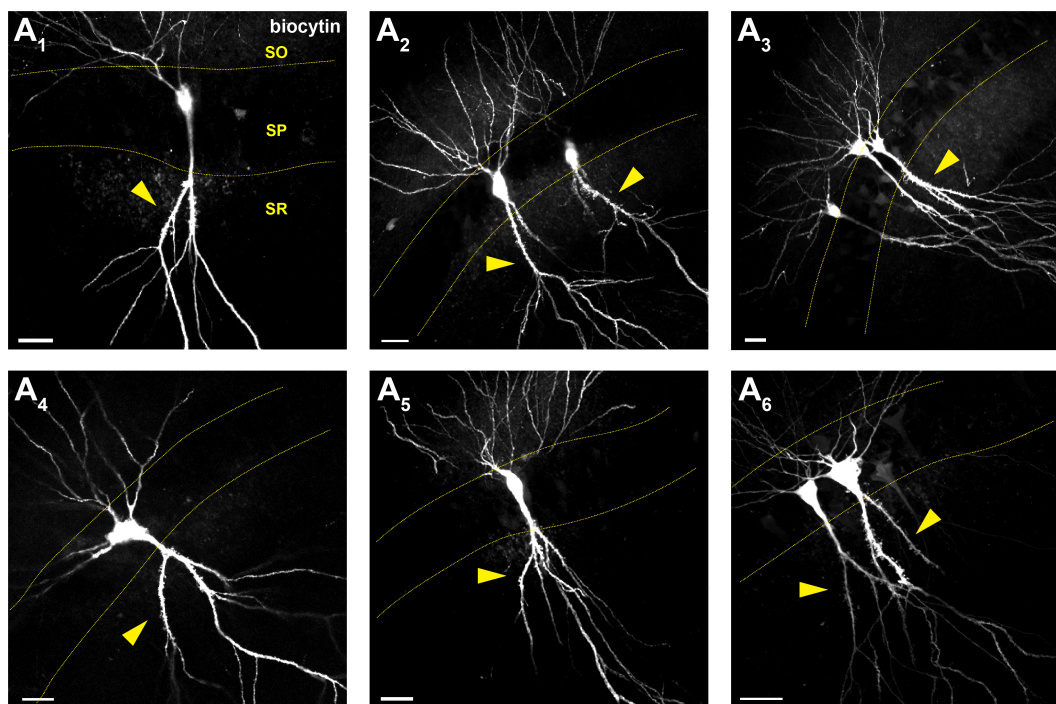


Figure S4

Figure S4, related to Figure 3, Figure 5, Figure 6, Figure S2, and Figure S7. An optogenetic strategy using the Amigo2-Cre mouse line to investigate CA2 PC synaptic output in hippocampal slices from control and PILO-SE mice. (A) AAV was injected bilaterally into the dorsal hippocampus of Amigo2-Cre mice to drive channelrhodopsin-2 (ChR2-eYFP) expression in dorsal CA2 PCs (see Methods). **(B)** Representative current clamp recording from a CA2 PC illustrating the effect of photostimulation (blue lines) delivered in 2 ms pulses, 15 times at a frequency of 30 Hz. **(C)** A simplified circuit diagram of CA3–CA2–CA1 hippocampal circuitry, in which CA2 PCs, like those in CA3, form both local recurrent excitatory axonal collaterals and projections to the CA1 region. CA2 preferentially excites CA1_{deep} PCs, and also back-projects to CA3. **(D)** A representative section from the dorsal hippocampus of AAV-injected Amigo2-Cre mice, showing ChR2-eYFP-expressing CA2 PCs near the site of viral injection. Scale bar is 200 μm . **(E₁ - E₃)** Immunohistochemistry showing the CA2 marker RGS14 (red) colocalized with ChR2-eYFP expression (green), demonstrating expression specificity in CA2 PCs. Yellow dashed lines indicate the approximate bounds of the CA2 subfield. Scale bar is 80 μm . **(F₁ - F₃)** CA2 PC axons project throughout the CA1 region and densely innervate CA1 PC basal dendrites in the SO. Scale bar is 150 μm . **(G₁ - G₃)** CA2 PC axonal collaterals branch throughout CA2 and distal CA3; only sparse projections are seen in proximal CA3. Scale bar is 150 μm . **(H)** A representative section from the intermediate portion (approximately the middle third) of the hippocampus from an AAV-ChR2-eYFP-injected Amigo2-Cre mouse, which contains longitudinally descending ChR2-eYFP-expressing CA2 axons originating from the dorsal hippocampus. Scale bar is 200 μm . **(I₁ - I₃)** In the intermediate hippocampus CA2 PCs (defined by RGS14 staining in red) did not express ChR2-eYFP expression but colocalized with ChR2-eYFP⁺ axon projections (green) from dorsal CA2 PCs. Yellow dashed lines indicate the approximate bounds of the CA2 subfield, identified by immunoreactivity for established selective markers of CA2 PCs (STEP, PCP4, or RGS14, see methods). Scale bar is 80 μm .

CA3a pyramidal cells



CA2 pyramidal cells

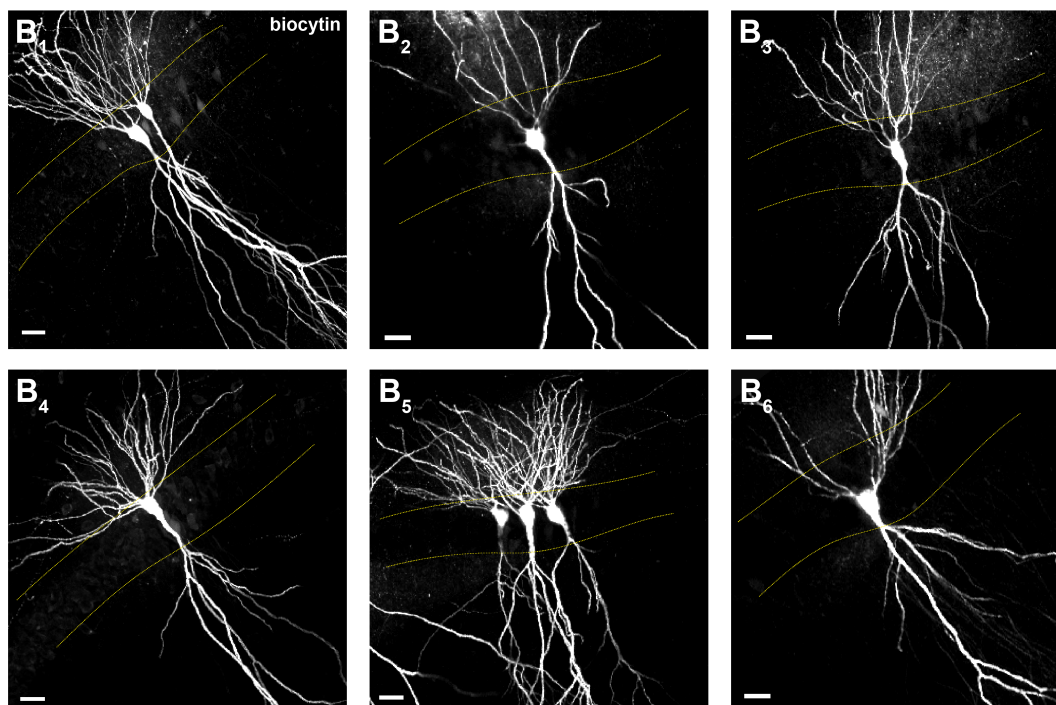


Figure S5

Figure S5, related to Figure 4. CA2 PCs can be distinguished from CA3 PCs by the absence of thorny excrescences. (A₁ – A₆) Representative CA3a PCs filled with biocytin in the course of whole-cell recordings. Thorny excrescences on the proximal apical dendrites are indicated by yellow arrowheads. **(B₁ – B₆)** Representative CA2 PCs filled with biocytin in the course of whole-cell recordings. No thorny excrescences are visible on the proximal apical dendrites. All scale bars are 30 μ m.

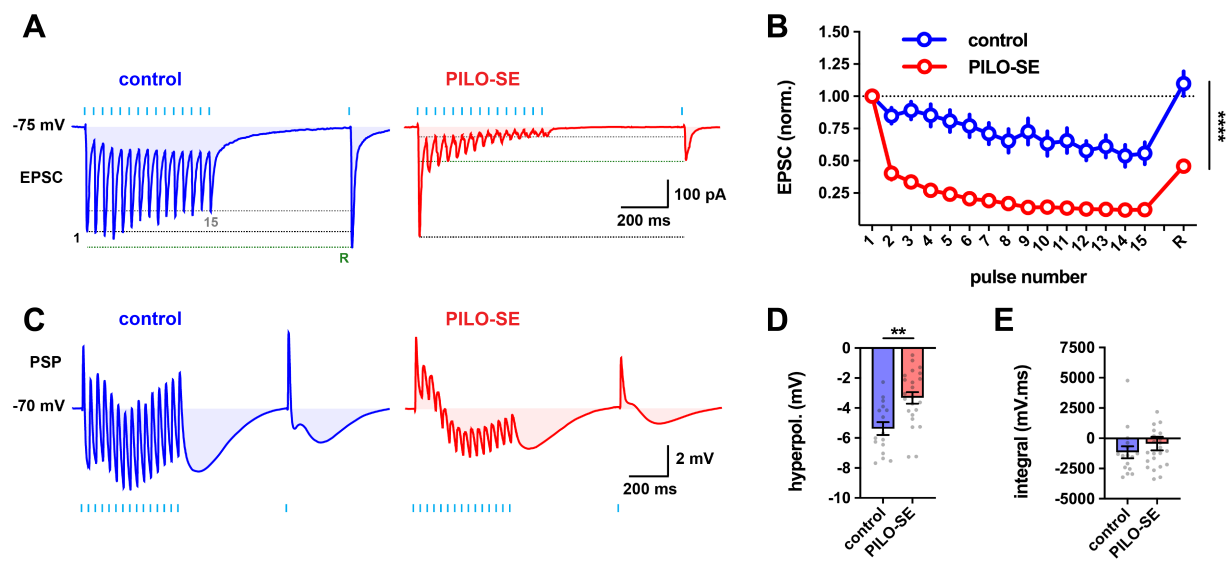


Figure S6

Figure S6, related to Figure 4. The granule cell mossy fiber input to CA2 PCs exhibited pronounced short-term depression following PILO-SE. (A) To examine short-term plasticity 15 light pulses (2 ms) were delivered at a frequency of 30 Hz, followed up by a single recovery pulse 500 ms after the train. Top, the blue lines indicate the timing of each 2 ms light pulse. Below, EPSCs in CA2 PCs from control and PILO-SE mice in response to the photostimulation train protocol. **(B)** In CA2 PCs from PILO-SE mice, the light-evoked EPSC exhibited a prominent short-term depression, which persisted to the recovery pulse. **(C - E)** In current clamp recordings from CA2 PCs from PILO-SE mice, the photostimulation train evokes a compound PSP with reduced hyperpolarization amplitude (D). However, the net integral of the train-evoked PSP is not significantly altered (E).

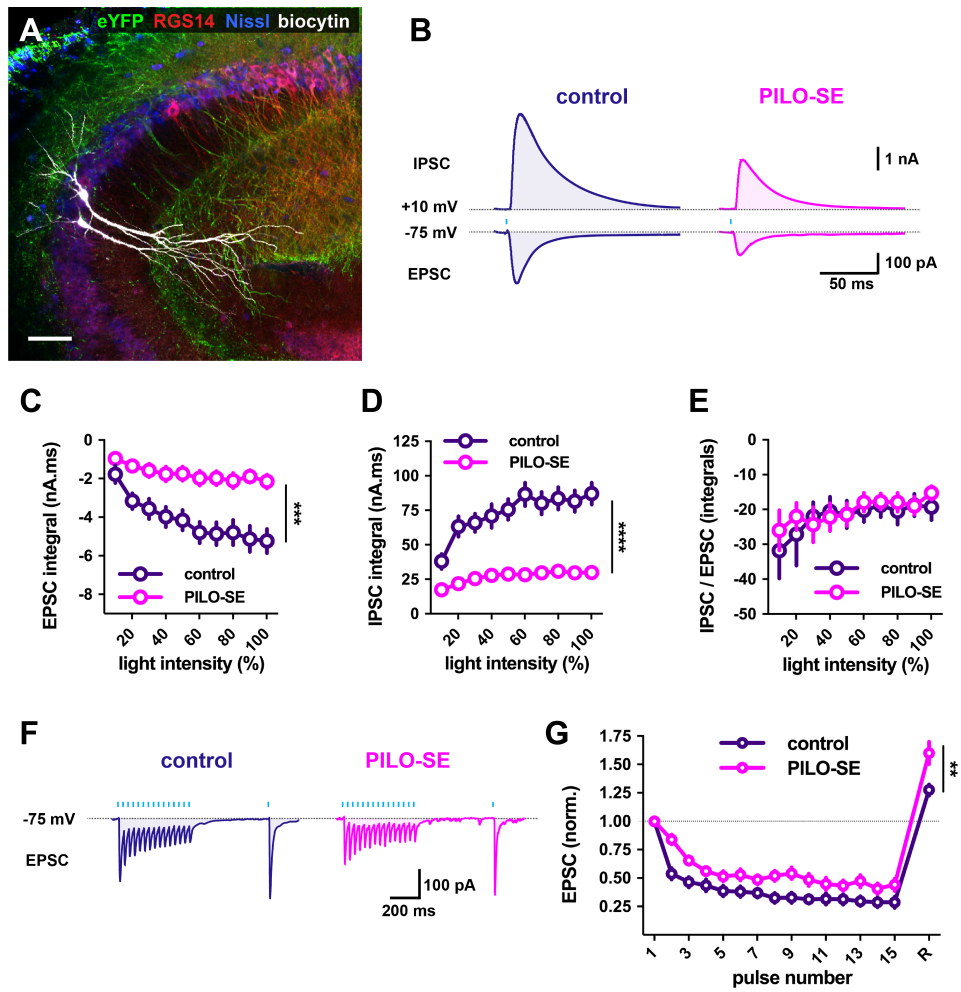


Figure S7

Figure S7, related to Figure 5 and Figure 6. The CA2 back-projecting circuit to CA3a is weakened in slices from PILO-SE mice. (A) A representative image of two biocytin-filled CA3a PCs (white) surrounded by Chr2-eYFP-expressing CA2 axonal collaterals visible in the SO and SR (green), with CA2 PCs labeled using RGS14 (red) and neuronal somata labeled using a Nissl stain (blue). Scale bar is 80 μm . **(B)** Representative light-evoked averaged EPSCs and IPSCs recorded from CA3a PCs voltage clamped at -75 mV and +10 mV, respectively, in hippocampal slices from control (left, dark purple) and PILO-SE (right, magenta) mice. **(C)** The integral of the light-evoked EPSC was significantly reduced in CA3a PCs from PILO-SE mice (two-way ANOVA; *** $P = 0.0004$; $n = 11$ cells from 3 control mice, 19 cells from 7 PILO-SE mice). **(D)** The integral of the light-evoked IPSC was significantly reduced in CA3a PCs from PILO-SE mice (two-way ANOVA; **** $P < 0.0001$; $n = 12$ cells from 3 control mice, 19 cells from 7 PILO-SE mice). **(E)** The ratio of the integrals of the light-evoked IPSCs and EPSCs in CA3a PCs was not significantly altered in slices from PILO-SE mice (two-way ANOVA; $P = 0.7831$; $n = 11$ cells from 3 control mice, 18 cells from 7 PILO-SE mice). **(F)** Representative EPSCs evoked by 30 Hz photostimulation, with 15 pulses followed after 500 ms by a single recovery pulse. **(G)** Measurement of normalized EPSC amplitude reveals reduced short-term depression in CA3a PCs from PILO-SE mice.

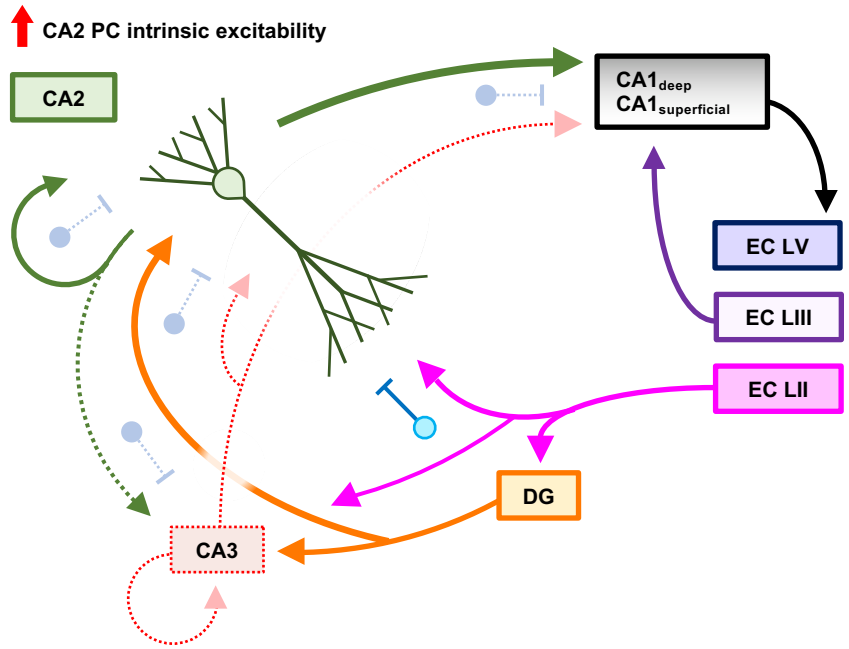


Figure S8

Figure S8, related to Figure 1, Figure 2, Figure 3, Figure 4, Figure 5, and Figure 6. A summary of alterations to CA2 circuits following pilocarpine-induced status epilepticus.

Reductions in GABAergic inhibition were observed in pathways examined, except for the entorhinal cortex projections in SLM to CA2. Dashed lines and faded color indicates a functional deficit in inhibitory circuits, which may result from a number of mechanisms including interneuronal depletion or reduced presynaptic neurotransmitter release. Dashed lines in the CA3 connections reflect the loss of CA3 PCs that often results from PILO-SE. We found an increased strength of the excitatory mossy fiber inputs from DG granule cells to CA2 PCs and from CA2 PCs to CA1 PCs, as well as increased intrinsic excitability of CA2 and CA1 PCs.

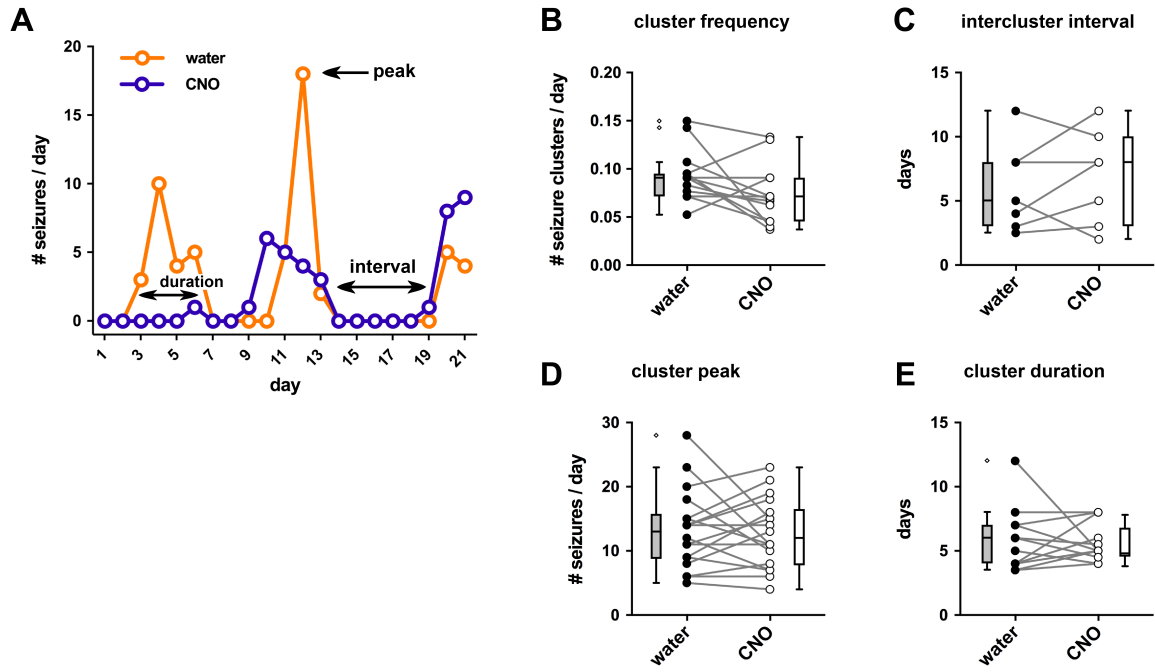


Figure S9

Figure S9, related to Figure 7 and Figure 8. CA2 silencing did not alter seizure clustering.

(A) A representative example of seizure clustering in one mouse expressing hM4D(Gi)-mCherry in CA2 PCs, with three weeks of daily seizure counts in absence of CNO (orange) and during delivery of CNO (purple). **(B)** The frequency of seizure clusters was not reduced by CNO treatment (paired t-test; $t = 1.941$, $df = 14$, $P = 0.0727$; $n = 15$ mice). **(C)** The intercluster interval was not altered by CNO treatment (paired t-test; $t = 0.7597$, $df = 6$, $P = 0.4762$; $n = 7$ mice). **(D)** The peak daily seizure total was not altered by CNO treatment (paired t-test; $t = 0.3575$, $df = 17$, $P = 0.7251$; $n = 18$ mice). **(E)** The cluster duration was not altered by CNO treatment (paired t-test; $t = 0.26731.941$, $df = 12$, $P = 0.7938$; $n = 13$ mice).